SRTTU
Journal of Computational and Applied Research in Mechanical Engineering
jcarme.sru.ac.ir
JCARME
ISSN: 2228-7922

Research paper

Investigating the performance of tubular direct ammonia IT-SOFC with temkin- pyzhev kinetic model using machine learning and CFD

M. Keyhanpour[a] and M. Ghassemi[a,*]

[a] *Department of Mechanical Engineering, Khaje Nasir Toosi University of Technology, Tehran, Tehran, 1999143344, Iran*

Article info:

Article history:

Received: 23/08/2024
Revised: 15/02/2025
Accepted: 25/01/2025
Online: 00/00/0000

Keywords:

Solid oxide fuel cell,
CFD,
Machine learning,
Ammonia,
Temkin-pyzhev.

[*]Corresponding author:
ghasemi@kntu.ac.ir

Abstract

Researchers encounter difficulties in producing clean energy and addressing environmental issues. Solid oxide fuel cells (SOFCs) present a promising prospect to the growing demand for clean and efficient electricity due to their capacity to convert chemically stored energy into electrical energy directly. In enhancing this technology, ammonia is employed as a cost-effective and carbon-free fuel with convenient transport capabilities. Efficiently predicting the performance of a system in relation to its operating environment has the potential to expedite the identification of the optimal operating conditions across a broad spectrum of parameters. For this purpose, the performance of intermediate temperature solid oxide fuel cell (IT-SOFC) with inlet ammonia fuel is predicted utilizing machine learning, which is efficient in time and cost. Initially, the system is simulated with computational fluid dynamics finite element code to generate data for training machine learning algorithms (DNN, RFM and LASSO regression), followed by an evaluation of the predictive accuracy of these algorithms. The analysis demonstrates that the three examined algorithms exhibit sufficient accuracy in predicting the performance of the introduced solid oxide fuel cell (SOFC) system, all surpassing a 95 percent threshold. RFM and DNN exhibit the most accurate predictions for the maximum temperature and power density of fuel cells, respectively.

1. Introduction

The energy crisis and environmental issues have had serious consequences for human life over the past few decades. The increase in energy demand, greenhouse gas emissions and limited fossil fuel resources have prompted research efforts to develop sustainable and renewable energy sources. One promising option is solid oxide fuel cells (SOFCs), which can directly convert chemical energy into electricity. These cells have gained widespread acceptance due to their advantageous characteristics, including versatility in utilizing various fuels, high efficiency, and lack of reliance on precious metals [1].

They are appropriate for use in mobile and stationary applications, catering to both small and large-scale systems [2, 3]. Hydrogen is an ideal fuel for SOFCs due to its high

electrochemical synthesis and the generation of only water vapor as the chemical reaction product. However, challenges associated with hydrogen fuel, such as its low energy density in the gaseous state, complicated storage, and limited portability, have led to the consideration of ammonia as a viable substitute fuel [4].

Ammonia's cost-effectiveness, ease of transport and storage, lack of carbon emissions and ability to be easily converted into a liquid form with a volume density approximately 1.4 times that of liquid hydrogen, have positioned it as a superior option for utilization in SOFCs as fuel [5-7]. Research has shown that the performance of ammonia-fed solid oxide fuel cells is influenced by various factors, including ammonia concentration, operating temperature, catalysts and materials, cell design, and configuration, fuel pre-processing and even system integration [8-20].

The solid oxide fuel cell is classified as a high-temperature fuel cell, with operating temperatures typically ranging from 500 to 900 degrees Celsius. An additional strategy for the advancement of the solid oxide fuel cell industry is to operate it at an intermediate temperature level. For this purpose, instead of employing the high-temperature kinetic model developed by Tamaro [14], it is imperative to utilize a kinetic model tailored for intermediate operating temperatures. The Temkin-Pyzhev kinetic model, as introduced by Vilekar et al. [21] in 2012, is a pertinent framework for simulating ammonia decomposition under these operating conditions.

Numerous investigations have been conducted to simulate appropriate models for comprehending the performance of SOFCs and predicting their behavior.

These studies involve a variety of models, ranging from zero-dimensional to three-dimensional, providing valuable insights into different aspects of the topic. They address fundamental factors including specific reactions [22], mass transport, porous media transport, and heterogeneous chemistry [23]. Additionally, they delve into more intricate data, including dynamic behavior [24, 25], spatial temperature, gas species, current density, and potential distribution [26].

Commercial CFD (computational fluid dynamics) software programs have commonly been utilized to analyze the behaviour of solid oxide fuel cells, necessitating precise selection of boundary conditions, and design parameters related to mass, heat and charge transport. While this approach offers accurate results for a specific fuel cell sample with unique characteristics, it may not be applicable to other fuel cell variations with differences in parameters such as electrode thickness and cell porosity. Therefore, the CFD software-based model requires additional time to simulate each distinct condition individually.

To address this issue efficiently and prevent unnecessary expenditure of time and resources, machine learning algorithms-- a component of artificial intelligence-- have been employed. Machine learning is a mathematical technique that utilizes statistical algorithms to analyze sample or training data to predict and estimate system behaviour under varying circumstances [27]. This methodology demonstrates reliable accuracy in the field of fuel cells and facilitates result optimization [28-30]. Moreover, it expedites computational procedures.

In 2002, Arriagada et al. [31] predicted the parameters of a planar solid oxide fuel cell using an artificial neural network (ANN). In this research, fuel cell outputs, such as electric current density and final temperature, were determined through the analysis of input data, including fuel composition, inlet gas temperature, voltage, and flow rate.

The network was trained using the Levenberg–Marquardt algorithm, an enhanced version of the backpropagation (BP) algorithm, resulting in accurate generation of output data. Subsequently, Milewski et al. [32] explored the performance of a solid oxide fuel cell with hydrogen fuel and a mixture of nitrogen and oxygen as oxidizers using an artificial neural network (ANN).

The effective parameters considered in this study included the temperature of the fuel cell, the thickness of the electrolyte and anode, the porosity of the anode, and the composition of the fuel and oxidizer mixtures. The findings suggested that employing a limited number of neurons in the neural network led to discrepancies, whereas utilizing the optimal number of neurons enabled the prediction of electric current density with appropriate accuracy and high speed. Chaichana et al. [33] examined a direct internal reforming solid oxide

fuel cell (SOFC) using neural network technology.

Their study focused on a fuel input comprising methane, carbon monoxide, carbon dioxide, hydrogen, and water vapor, employing the backpropagation (BP) methodology to forecast the current density output. The results revealed that elevating the operating temperature, pressure, steam/carbon ratio, and degree of pre-reforming positively impacted the efficiency. Conversely, the influence of the inlet fuel molar flow rate exhibited a contrasting trend. Furthermore, the fuel cell's electrical characteristics can be accurately estimated using the optimal structure of the neural network.

In another study conducted by Xu et al. [34], the combination of multi-physics simulation and deep learning (DL) was considered to predict and optimize the performance of SOFCs. They utilized hydrogen fuel, water vapor, and laboratory data to perform artificial intelligence calculations, resulting in an acceptable prediction of SOFC performance.

The performance of hydrogen-fueled SOFC was analyzed through Random Forest (RF) and Support Vector Machine (SVM) algorithms by Iskenderoglu et al. [35]. The performance of the fuel cell was assessed by 1122 laboratory data involving various mixtures of input fuel and operating temperature. The results showed that the electric current density of the fuel cell at 0.52 seconds could be predicted with errors of 1.97% and 0.92% using the RF and SVR methods, respectively.

Three different methods were employed in the study by Ba et al. [36] to predict the efficiency of fuel cells: RHNN, RHNN-GWO, and RBF. Based on the results, RHNN-GWO demonstrated higher accuracy in predicting SOFC performance compared to the other two algorithms. Li et al. [37] utilized deep reinforcement learning to effectively manage and analyze the solid oxide fuel cell performance, which was operated with hydrogen fuel at a temperature of 1273 K, at different voltage levels.

The purpose of this simulation was to maintain a constant output flow of the fuel cell. In addition, the optimal performance of the solid oxide fuel cell was identified by Jia et al. [38] through a fusion of Elman Neural Network (ENN) and Quantum Pathfinder algorithm (QPF). The findings indicated that the employed approach exhibited lower error rates compared to the ENN-PF and GWO-RHNN techniques and could accurately predict the power of fuel cell.

Subotić et al. [39] applied artificial neural networks (ANNs) to predict SOFC performance, emphasizing prediction accuracy. By expanding the training data to encompass diverse operating conditions and increasing the dataset size, ANNs can predict performance for different fuel mixtures and operating scenarios, potentially averting failures and extending system lifetime. In a subsequent study, Mütter et al. [40] focused on optimizing SOFC operational parameters using an ANN and a genetic algorithm (GA). The combination of ANN-GA accelerates predictions significantly while upholding accuracy, facilitating the commercialization of SOFCs. Finally, Tofigh et al. [41] introduced a novel model, HY-CNN-NARX, capable of identifying the transient dynamic behavior of SOFCs.

This model combines convolutional neural network (CNN) with a nonlinear autoregressive exogenous (NARX) network. Experimental data from lab-scale SOFCs validated the model, demonstrating improved accuracy and faster execution times compared to conventional models.

Considering the growing demand for energy and environmental crises such as climate change and global warming, it is essential and vital to use sustainable and carbon-free fuels to replace fossil fuels. In this regard, the fuel cell with ammonia fuel is a promising option [7]. This is because ammonia can be easily produced, transported and distributed compared to hydrogen. Also, as a carbon-free fuel, it does not emit environmental pollutants at the point of consumption (net zero emissions) compared to fossil and traditional fuels [42, 43].

According to the literature, no previous research has been conducted on three-dimensional tubular SOFC modeling with ammonia fuel at intermediate operating temperature using CFD simulation. The primary objective of this study is to perform a comparative investigation on various machine learning algorithms to predict the performance of the proposed SOFC systems.

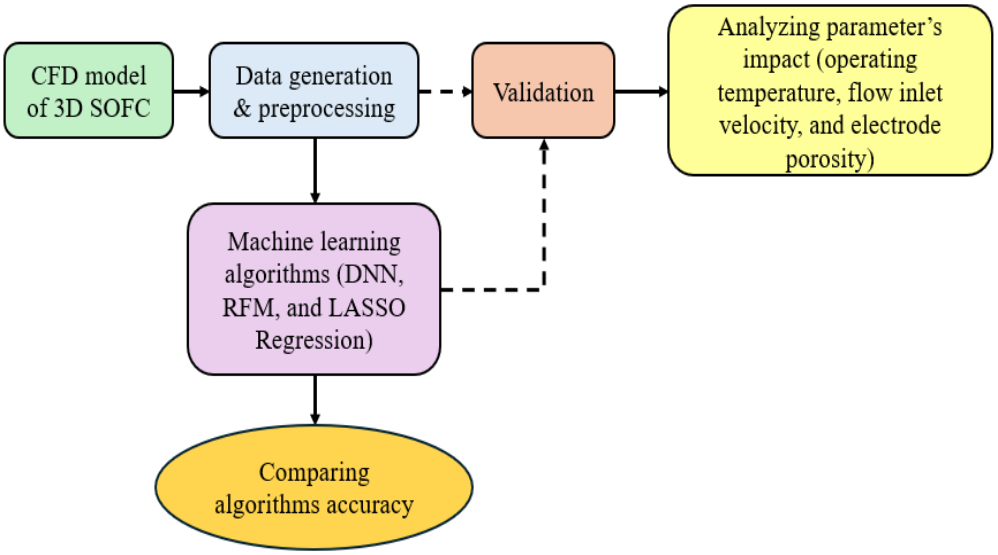

Fig. 1. Simplified workflow of SOFC performance prediction.

The steps undertaken for this research are outlined in Fig. 1.
Initially, a CFD model is employed to generate a dataset, examining the impacts of operating temperature, flow inlet velocity, and electrode porosity on SOFC efficiency. After preprocessing, this data is used to configure and train machine learning algorithms (DNN, RFM, LASSO Regression).
Both the CFD-simulated and machine learning models are validated against the study conducted by Ranasinghe and Middleton [44]. Subsequently, the accuracy of different machine learning algorithms is compared to determine the most effective approach for predicting the performance of the introduced SOFC system.

2. Model description

This study investigates the three-dimensional structure of a tubular solid oxide fuel cell, as depicted in Fig. 2. The fuel cell receives ammonia fuel and air flow through its anode and cathode channels, respectively.
The decomposition of ammonia fuel into hydrogen and nitrogen occurs after penetrating the anode channel. The simulation is based on the premise of operating at intermediate working temperatures, where the chemical reaction rate (r_{NH_3}) for ammonia decomposition is evaluated using the Temkin-Pyzhev relationship [45].

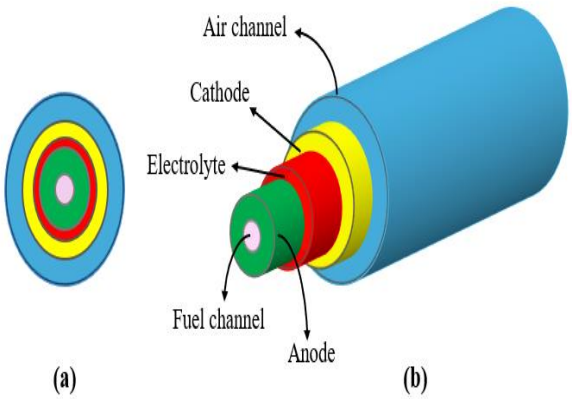

Fig. 2. Configuration of 3D tubular SOFC a) front view b) layers.

$$r_{NH_3} = 6 \times 10^7 exp\left(-\frac{95600}{RT}\right)\left(\frac{p_{NH_3}^2}{p_{H_2}^3}\right)^{0.209} \quad (1)$$

In Eq. (1), P_{NH_3} and P_{H_2} represent the partial pressures of ammonia and hydrogen, respectively. Meanwhile, T and R denote the reaction temperature and the universal gas constant, respectively. After the decomposition of ammonia within the porous medium of the

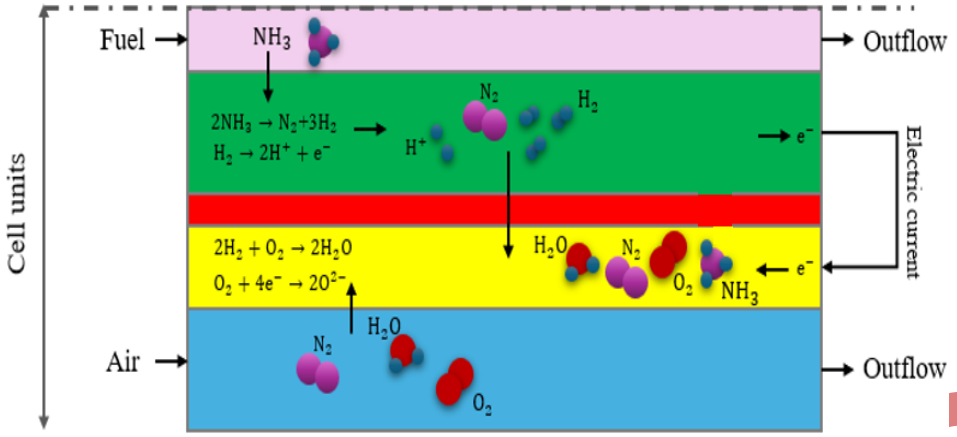

Fig. 3. Chemical and electrochemical reactions of ammonia fuelled SOFC.

Anode, the generation of an electric current occurs through the conduction of protons from the electrolyte to the cathode during the electrochemical reaction. In Fig. 3, the species, as well as the chemical and electrochemical reactions in cell units, are shown in two dimensions.

Table 1 displays the thickness of each layer within the introduced SOFC system.

Table 1. The dimensions of various components of the tubular SOFC.

Parameters	Size (mm)
Fuel channel radius	0.175
Anode thickness	0.35
Electrolyte thickness	0.01
Cathode thickness	0.06
Air channel thickness	0.35
Fuel cell length	10

2.1. Model equations

To accurately simulate and analyze the solid oxide fuel cell, it is crucial to integrate and address the fundamental equations governing this system. These equations include electrochemical equations, mass transfer, thermophysical and fluid characteristics of mixtures, fluid flows and energy. These equations are solved in the steady state and the species within the SOFC are assumed to behave as ideal gases.

The fluid behavior equation incorporates compressibility for accurate modeling, and the thermodynamic properties of species and mixtures are characterized by accounting for the influence of mole fraction, temperature, and pressure.

The investigation of fuel and air flow within the anode and cathode channels is conducted by applying the principles of continuity and momentum equations, while considering a compressible (Mach number < 0.3) and laminar fluid.

$$\nabla.(\rho V) = 0 \tag{2}$$

$$\rho(V.\nabla)V = \nabla.[-pI + K] + F \tag{3}$$

$$K = \mu(\nabla V + (\nabla V)^T) - \frac{2}{3}\mu(\nabla.V)I \tag{4}$$

In Eqs. (2-4), the variables V, ρ, F, p and μ represent the velocity field, fluid density, applied volumetric force to the fluid, pressure field, and dynamic viscosity of the fluid flow mixture, respectively. The Darcy-Brinkman relation is employed to address the preservation of momentum in fluid flow within porous media. Consequently, the equations defining the fluid flow within the porous medium of the electrodes are as follows:

$$\nabla.(\rho V) = Q_m \tag{5}$$

$$\frac{1}{\varepsilon_p}\rho(V.\nabla)V\frac{1}{\varepsilon_p} = \nabla.[-pI + K_1] + F - \left(\mu\kappa^{-1} + \frac{Q_m}{\varepsilon_P^2}\right)V \quad (6)$$

$$K_1 = \frac{1}{\varepsilon_p}\mu(\nabla V + (\nabla V)^T) - \frac{2}{3}\mu\frac{1}{\varepsilon_p}(\nabla.V)I \quad (7)$$

The quantities Q_m, ε_p and κ represent mass source, medium porosity, and permeability, respectively. The air flow includes water vapor, oxygen and nitrogen, and the incoming fuel flow is pure ammonia. After decomposition, the ammonia gas transitions into a mixture of nitrogen, hydrogen, and ammonia. To evaluate the transfer of these species based on the mixture's thermophysical and fluid properties, the Maxwell-Stefan equation is employed, as depicted below. R_i, ω_i and J_i are source term, mass fraction, and mass flux of species.

$$\nabla, J_i + \rho(V, \nabla)\omega_i = R_i \quad (8)$$

To calculate the mass flux diffusion parameter, the following equations are used, in which the symbols d_k, $D_{e,ik}$, f_e, τ_F, D_{ik}, x_k, M_n, and M_i represent diffusional driving force, effective binary diffusion coefficient, effective transport factor, tortuosity, binary diffusion coefficient, molar fraction of species, average molar mass and molar mass of species, respectively.

$$J_i = -(\rho\omega_i\sum_k D_{e,ik}d_k) \quad (9)$$

$$D_{e,ik} = f_e(\varepsilon_p, \tau_F)D_{ik} \quad (10)$$

$$d_k = \nabla x_k + \frac{1}{p}[(x_k - \omega_k)\nabla p] \quad (11)$$

$$x_k = \frac{\omega_k}{M_k}M_n \quad (12)$$

$$M_n = (\sum_i \frac{\omega_i}{M_i})^{-1} \quad (13)$$

The quantity f_e is a function of two values: porosity and tortuosity, which in this research is determined by the assumption of Bragman's model regarding the effective transport factor.

$$f_e = \frac{\varepsilon_p}{\tau_F} \quad (14)$$

$$\tau_F = \varepsilon_P{}^{-\frac{1}{2}} \quad (15)$$

The ionic and electric currents produced as a result of electrochemical reactions are calculated using the charge conservation equation as follows:

$$-\nabla.(\sigma_e\nabla\phi_e) = j_e \quad (16)$$

$$-\nabla.(\sigma_i\nabla\phi_i) = j_i \quad (17)$$

In Eqs. (16, 17), σ_e, σ_i, ϕ_e, ϕ_i refer to electron and ion conductivity, and electron and ion potentials, respectively. The parameters j_e and j_i identify the source of electric and ionic currents that are produced or consumed in fuel cell. The Butler-Volmer equation is employed to establish the correlation between the current and the Additional activation potential. In this relation, A_a, i_0, α_a, α_c, F, and η represent electrochemical active surface per unit volume, exchange current density, anodic and cathodic charge transfer coefficient, Faraday constant and excess potential, respectively.

$$j = A_a i_0(C_r\, exp\left(\frac{\alpha_a F}{RT}\eta\right) - C_0\, exp\left(\frac{\alpha_c F}{RT}\eta\right)) \quad (18)$$

The terms C_r and C_0 are the reduced and oxidized ratios of species to reference values, respectively. The η parameter is defined as follows:

$$\eta = \phi_e - \phi_i - V_{ocv} \quad (19)$$

V_{ocv} is the open circuit potential, which is zero in the anode catalytic layer. The value of this parameter in the cathode layer is determined by the following relation:

$$V_{ocv} = 1.253 - 0.00024516T + \frac{RT}{2F}ln\frac{p_{H_2}(p_{O_2})^2}{p_{H_2O}} \quad (20)$$

The energy equation is used to compute the temperature distribution of gaseous fluids within fuel and air channels, as well as in porous electrode environments that encompass both solid and fluid components in the solid oxide fuel cell systems.

$$\rho C_p V.\nabla T + \nabla.\left(-k_{eff}\nabla T\right) = Q_h \quad (21)$$

In Eq. (21), C_p, T, Q_h and k_{eff} are respectively the specific heat capacity of gas mixture, temperature, heat source resulting from chemical and electrochemical reactions and effective thermal conductivity. k_{eff} is defined as follows:

$$k_{eff} = \varepsilon_p k_f + (1-\varepsilon_p)k_s \quad (22)$$

The heat source includes the heat produced or consumed in various parts of the fuel cell, which is defined as follows:

$$\begin{aligned} Q_e &= {\sigma_i}^{el}\left(\nabla {\phi_e}^{el}\right)^2 + Q_{elec} \\ Q_c &= {\sigma_i}^{c}(\nabla {\phi_e}^{c})^2 + {\sigma_e}^{c}(\nabla {\phi_e}^{c})^2 + i\eta \\ Q_a &= {\sigma_i}^{a}(\nabla {\phi_e}^{a})^2 + {\sigma_e}^{a}(\nabla {\phi_e}^{a})^2 + i\eta \\ &\quad + Q_{chem} \end{aligned} \quad (23)$$

The heat generated by electrochemical reactions, ohmic heat loss, excess potential heat loss, and chemical reaction resulting from the decomposition of ammonia are denoted by Q_{elec}, ${\sigma_i}^{el}\left(\nabla {\phi_e}^{el}\right)^2$, $i\eta$, and Q_{chem}, respectively, in Eq. (23). In this study, the thermal enthalpy of the endothermic reaction of ammonia decomposition is considered equal to 46 *kJ/mol*. To analyze the problem, the aforementionedequations are defined, coupled, and solved using a computational fluid dynamics code implemented based on the finite element method [46].

2.2. Machine learning algorithms

The essential information needed to train practical, and well-known machine learning models, including Deep neural network (DNN), Random Forest (RF), and LASSO regression [47], is obtained through numerical simulation results. A DNN is a statistical method that draws inspiration from biological neural networks. It consists different components, including the input layer, hidden layers, and an output layer. Each layer contains multiple processing units known as neurons. These neurons receive inputs, or information, from other neurons through specific connection weights. In the middle-hidden layers, the information received from the input layer is processed using an activation function. Each neuron receives all information from the previous layer. The simplified DNN algorithm is illustrated in Fig. 4. [48].

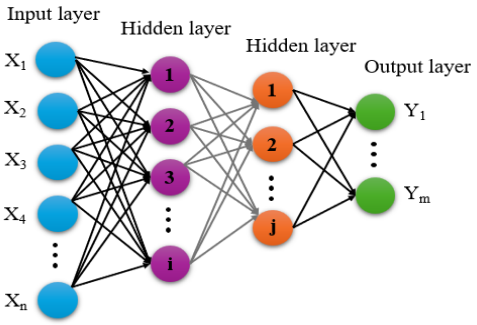

Fig. 4. Simplified structure of deep neural network algorithm.

DNN selected for its ability to model complex non-linear relationships via deep layers, outperforming shallow networks in capturing multi-scale dependencies. Chosen over simpler networks (e.g., ANN) due to higher accuracy in high-dimensional data.

To find the optimal mode of the network, various modes have been used for data analysis. Four activation functions for data processing, including the rectified linear unit (ReLU), identity, logistic, and hyperbolic tangent, are considered. In the neural network, each neuron can have a special weight and importance in predicting the objective function.

The calculation and optimization of the weight of each neuron is performed using a solver. In this research, the effects of three common solvers, including the Limited- Memory Broyden–Fletcher–Goldfarb–Shanno algorithm (LBFGS) which belongs to the family of the quasi- Newton Method, Stochastic Gradient Descent (SGD), and Adaptive Moment Estimation Method (ADAM), are examined. Eighty-five percent of the data is allocated for

training the machine and the rest is used for testing the machine.
The Random Forest algorithm creates multiple decision trees during the training phase.
Each tree is constructed by utilizing a random subset of the dataset to evaluate a random subset of features within each partition, as shown in Fig. 5. This incorporation of randomness introduces diversity among the individual trees, reducing the risk of overfitting and improving overall prediction performance. During the prediction phase, the algorithm combines the results of all the trees, by either using voting (for classification tasks) or averaging (for regression tasks).

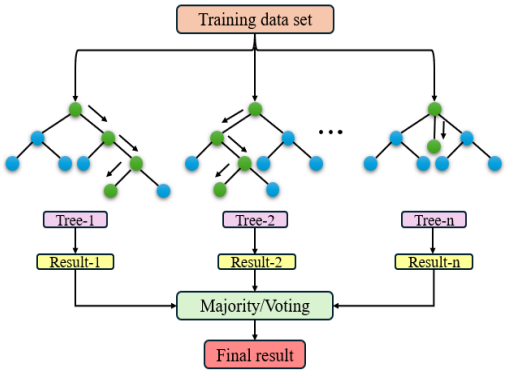

Fig. 5. Simplified structure of random forest model.

RF Preferred over other tree-based like decision tree for its robustness to overfitting in moderate datasets (601 cases) and inherent feature importance analysis. Its ensemble approach handles variable interactions better than single decision trees.
LASSO regression is a widely used algorithm in statistics and machine learning to perform feature selection and regularization. It operates by adding a penalty term, typically the L1 norm of the coefficients, to the ordinary least squares (OLS) regression loss function, which constraining the sum of the absolute values of the coefficients.
This encourages sparsity in the coefficient vector, leading to feature selection by shrinking less important coefficients to zero. By effectively reducing the number of predictors, LASSO regression can improve model interpretability, reduce overfitting and enhance prediction accuracy.
The algorithm is particularly useful when dealing with high-dimensional datasets where there are potentially many irrelevant or redundant features [49]. Also, LASSO Chosen over standard linear regression for its L1 regularization, which automates feature selection (e.g., isolating inlet temperature's dominance) while penalizing irrelevant variables, unlike non-regularized regression prone to overfitting.
The target parameters for predicting SOFC performance with machine learning algorithms are power density and maximum temperature of the fuel cell. To achieve this objective, various input parameters have been selected, that can vary and impact the target parameters. These input parameters include the initial temperature of the fuel cell, the porosity levels of both the anode and cathode, as well as the fuel and air flow velocities.
The applied voltage of the fuel cell for calculating different modes is set at 0.7 V. After modifying the input parameters, the governing equations and output parameters are calculated. A comprehensive analysis has been conducted, encompassing a total of 601 distinct modes.

3. Results and discussion

According to CFD modeling results, the temperature is highest at the fuel cell inlet and gradually decreases as it progresses through the fuel cell. This temperature reduction results from the endothermic ammonia decomposition reaction. The maximum temperature, maximum current, and power of the fuel cell are directly related to the operating temperature and the input flow velocities. The temperature of the fuel cell is not significantly influenced by the porosity of the electrodes; however, it does result in a reduction in both the maximum power and current of the fuel cell.

3.1. Model validation

To analyze the problem and generate the necessary data, the thermodynamic properties of species, mixtures and the conservation equations of mass, momentum, energy, electric charge and species have been defined in a finite element numerical code and coupled with each other. For the numerical solution of the equations and to

control instability, four steps are defined as follows:

- Solving the electric and ion flux conservation equations to calculate the electric current distribution
- Solving the continuity and momentum conservation equations to calculate pressure and velocity fields.
- Solving the species survival equation (Maxwell-Stefan) to calculate the species distribution
- Solving the energy equation to calculate the temperature field

After solving the mentioned steps, all the equations are solved simultaneously and coupled together. Additionally, based on the chemical and electrochemical reactions that cause changes in mole fraction, temperature, and pressure, thermophysical properties of species and mixture are calculated and used in the equations.

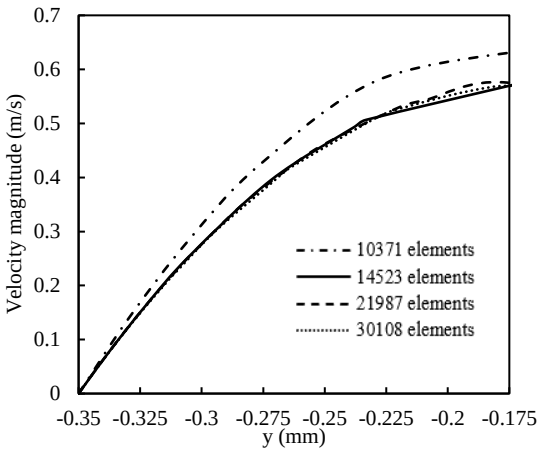

Fig. 6. Mesh independence.

To choose the appropriate mesh, the flow velocity in the air channel and along the transverse axis was analyzed in four computational grid modes. The results of the velocity magnitude in the four states are shown in Fig. 6. To choose the appropriate mesh, the flow velocity in the air channel and along the transverse axis was analyzed in four computational grid modes. The results of the velocity magnitude in the four states are shown in Fig. 6. Therefore, the computational grid consisting of 30,108 cells is used as the basis for subsequent calculations. The network includes 28852 triangular cells and 1256 quadrilateral cells, with more distribution in the contact area between electrolyte and electrodes. In total, the results obtained from the independence of the computing mesh and the average quality of the network more than 0.85 in the domain of the problem indicate the sufficient and appropriate accuracy of the numerical solution.

To solve the equations, it is necessary to define the boundary conditions. Therefore, to solve the conservation equations for energy and species, the boundary condition of constant value and dominance of convection are set at the inlet and outlet of the channels, respectively. To solve the electrochemical equation, the initial electric potential of the electrolyte and anode is zero while that the cathode is 0.7 V. To solve the continuity and momentum equations, assuming no-slip in the walls, the fully developed flow and constant pressure are defined at the inlets and outlets of the channels, respectively.

In the following, to validate our numerical model, we compare its results with those obtained by Ranasinghe and Middleton [44].

In this regard, the accuracy and precision of the numerical solution are compared with the research conducted by Ranasinghe and Middleton. In their study, the effects of counter and radial flows on the performance of a SOFC were investigated numerically. For this purpose, a three-dimensional geometry fueled by hydrogen was simulated at three different operating temperatures using COMSOL Multiphysics software. To solve the species and momentum conservation equations, specific boundary conditions were applied: the mass fraction and flow rate were set at the inlet of the channels, while the dominant convection over diffusion and constant pressure were defined at the outlet. Additionally, no-slip conditions and zero species diffusion were imposed at the walls of the channels and the interfaces between the electrolyte and electrodes.

In Fig. 7, the power density versus current density profiles from both studies are compared, demonstrating the reasonable accuracy of the numerical solution method employed in this study. The close agreement between the results validates the reliability of the computational approach used here [44].

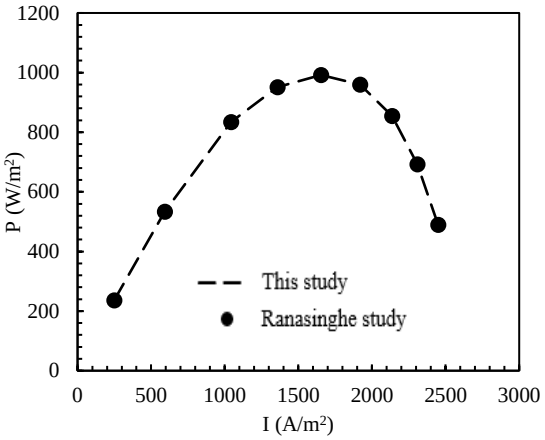

Fig. 7. The comparison of power density-electric current density diagram at present study and ranasinghe and middleton [44].

3.2. Numerical Modelling

After simulating and numerically verifying of solid oxide tubular fuel cell with ammonia as an inlet fuel and at intermediate working temperatures, the effects of changes in the input terms on the output terms is investigated and studied. The most effective input terms are the velocity of fuel and air flows, working temperature and anode and cathode porosity, while the output terms of the research are the power density and the maximum temperature of the fuel cell. Fig. 8 illustrates the quantitative and qualitative statistics of the selected input terms.

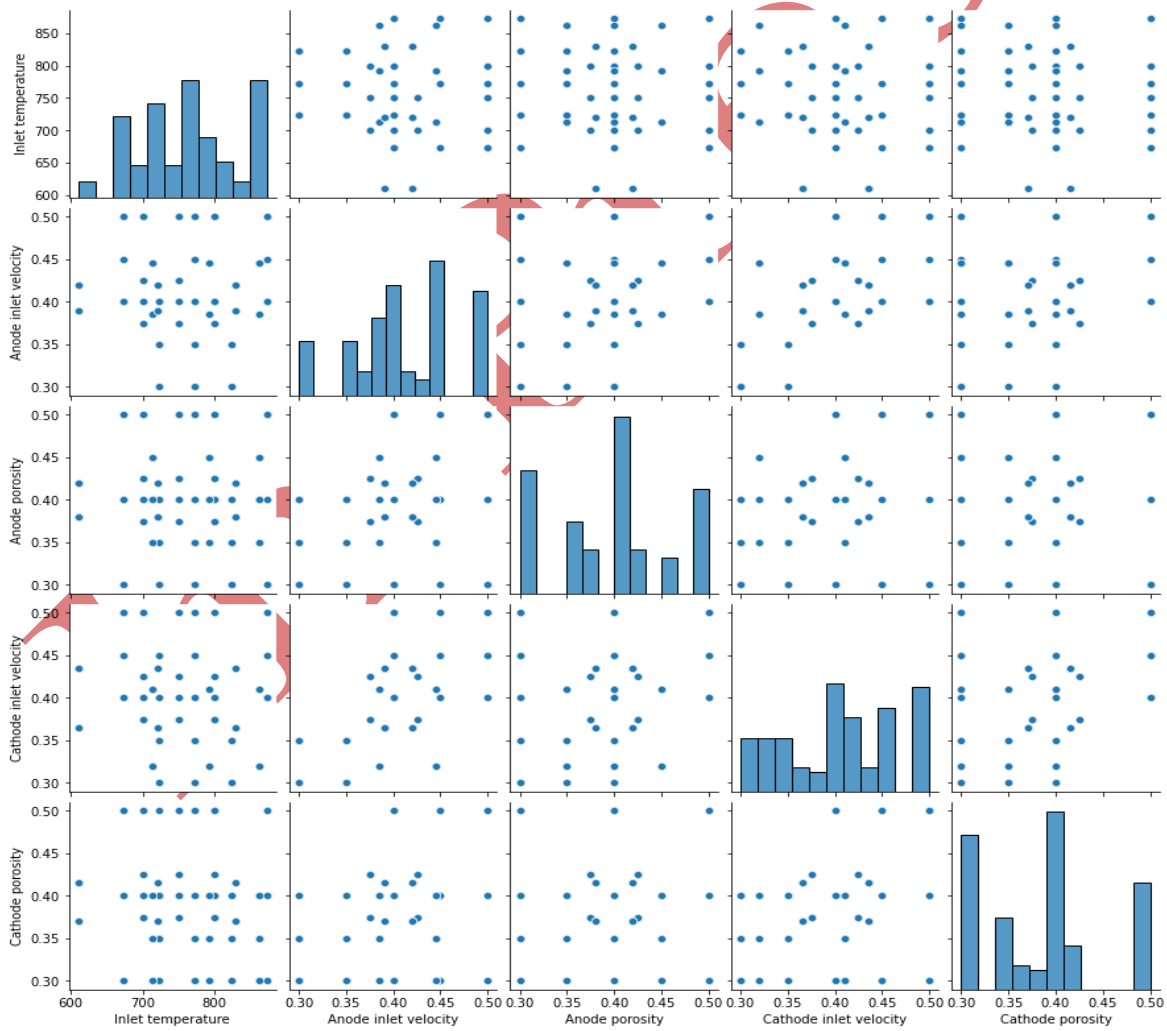

Fig. 8. Input parameters distribution.

As can be seen, the terms of electrodes porosity and the velocity of air and fuel flows have been selected in the conventional and practical range of 0.3 to 0.5 m/s. Also, the inlet temperature has been selected in the range of 610 to 873 K, according to the operating temperature range of the fuel cell and the Temkin-Pizhev kinetic model.

As can be seen in Fig. 8, the values of input parameters have been selected to include applicable values. For example, considering that the operating temperature of the fuel cell is average, major changes in temperatures have been studied around 773 K. Also, for other parameters, the values are chosen so that the entire range is properly covered. Fig. 9, displays the three-dimensional contour of temperature distribution and anode is lower than the air inlet channel and cathode, which is caused by the heat source of ammonia decomposition. Fig. 9 shows a temperature drop due to the endothermic reactions occurring along the fuel cell. It can also be observed that the temperature around the fuel inlet channel is lower.

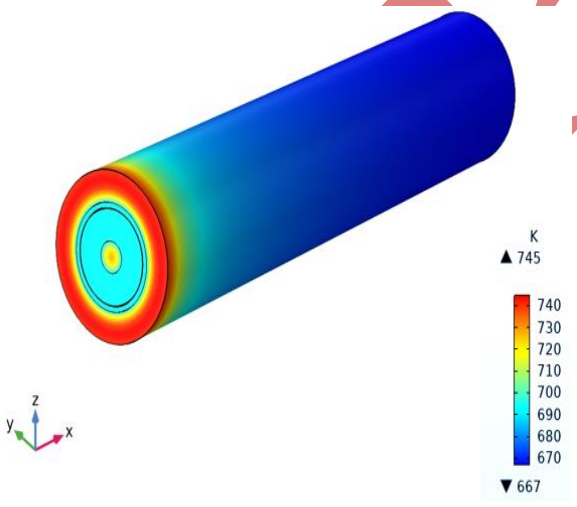

Fig. 9. 3D Temperature distribution.

Fig. 10 shows the mass fraction of ammonia at two different states of inlet temperature of 673 and 773 K. An increase in temperature results in a higher amount of ammonia decomposition.

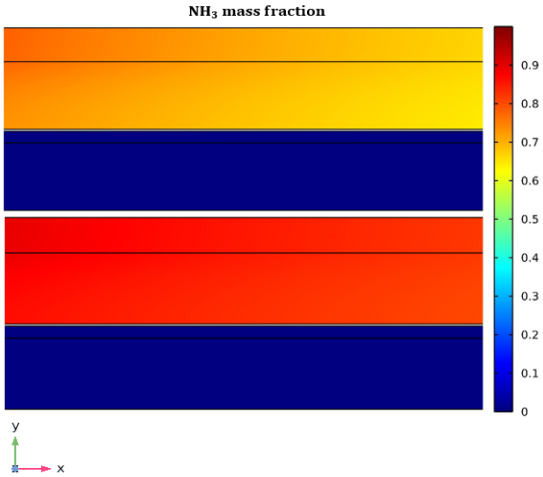

Fig. 10. 2D Ammonia mass fraction distribution.

Fig. 11 illustrates temperature variations along the center of the fuel cell assuming different electrodes porosity and air and fuel flows velocity. The base condition is assumed to have a porosity of 0.3 for the electrodes and a velocity of 0.3 m/s for the fuel and air inlet flows. In all cases, the inlet temperature is 673 K. The line graphs in Fig. 11 shows that changing the air flow velocity has a greater effect on the temperature change than other terms. It can also be seen that changing the porosity of the electrodes have the least effect on the temperature of the fuel cell compared to other terms.

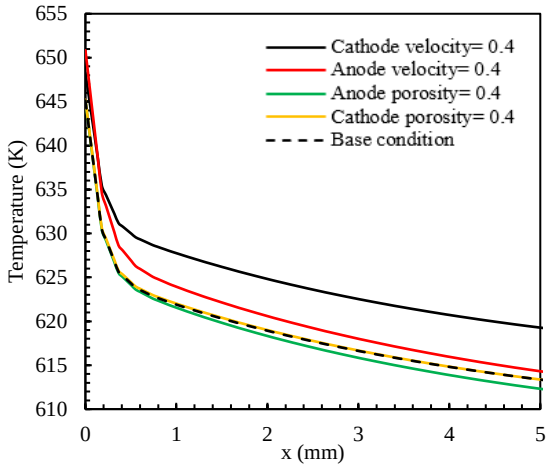

Fig. 11. Temperature changes in the direction of the center of the fuel cell assuming different states.

3.3. Comparison of machine learning algorithms

Upon completion of data generation from computational fluid dynamic codes, a python program is utilized to prepare the structure of machine learning algorithms. The correlation between the data sets is illustrated in Fig. 12 using the Pearson correlation coefficient (PCC). It is evident that the initial temperature of the fuel cell has a significant impact on its power density.

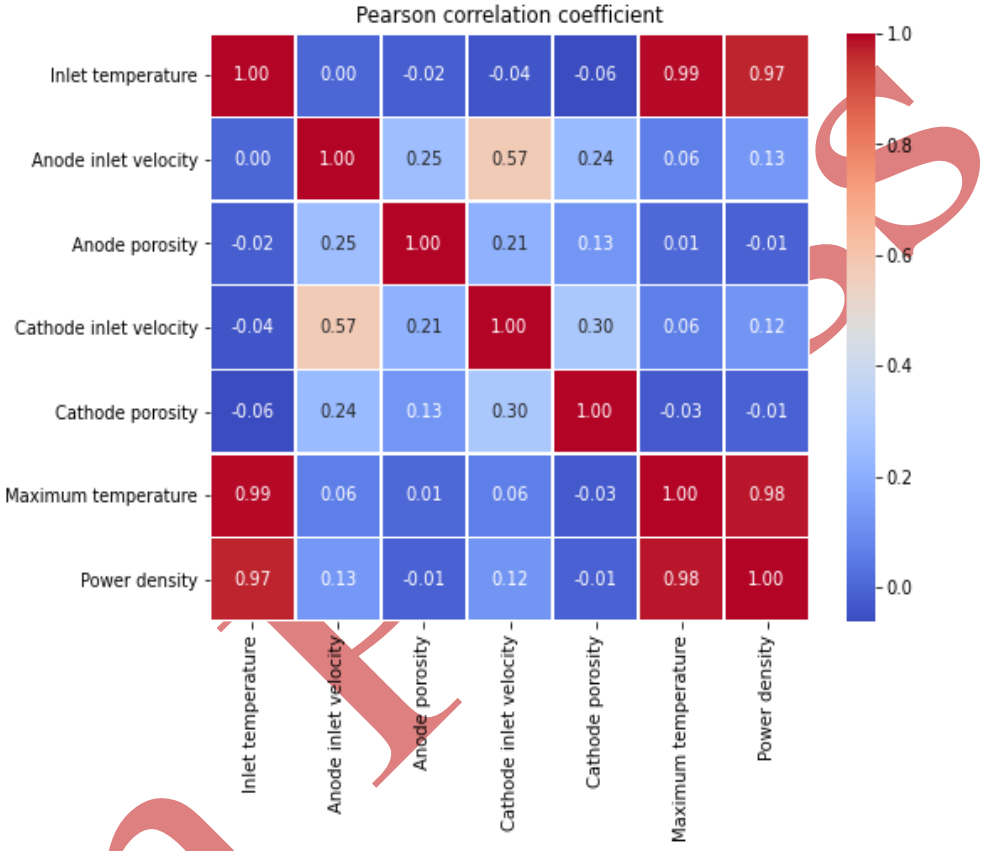

Fig. 12. Correlation between different data.

The correlation coefficients (P.C.C) of 0.99 and 0.97 between the inlet temperature and the maximum temperature and power density of the fuel cell, respectively, indicate a very strong positive linear relationship, signifying that the inlet temperature is a dominant factor influencing both the thermal and electrical performance of the fuel cell. The near-perfect correlation (0.99) between inlet temperature and maximum temperature highlights its critical role in controlling the fuel cell's thermal profile, while the strong correlation (0.97) with power density underscores its importance in optimizing power generation. These findings emphasize that Careful regulation of the inlet temperature is essential for enhancing fuel cell efficiency, guiding predictive modeling and informing design and control strategies to achieve optimal performance. Fig. 13 illustrates the relationship between variations in inlet temperature and fuel cell power density. It is evident that the inlet temperature has a direct relationship with the power density, and changes in temperature can lead to a significant variation in power density. Consequently, the effect of the inlet temperature on the target parameters is greater than other terms.

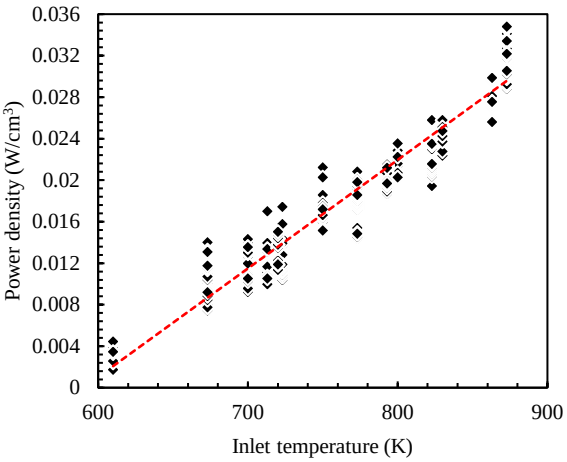

Fig. 13. Correlation between power density and inlet temperature.

Variations in the inlet temperature significantly influence the performance of an IT-SOFC ammonia fueled. Elevating the inlet temperature within the range of 610–873 K enhances the ammonia decomposition kinetics, promoting higher hydrogen yield. This increased hydrogen availability accelerates the electrochemical reactions governing proton and oxygen-ion formation at the electrodes, thereby amplifying the current density and power density of the cell. Furthermore, higher inlet temperatures improve charge transport phenomena, including ionic and electronic conductivity in the electrolyte and electrodes, while simultaneously enhancing mass transfer processes such as species diffusion and convective transport. The intensified electrochemical activity, however, increases heat generation through ohmic overpotential and electrochemically driven exothermic processes, such as hydrogen oxidation at the anode. In this regard, the maximum temperature of the fuel cell will increase.

Fig. 14 shows the performance of the artificial neural network in predicting two objective functions: including the maximum temperature and power density of the fuel cell. Actual and predicted values are plotted on the horizontal and vertical axes, respectively. In this context, the proximity of the points to the y=x line indicates the appropriate performance and accuracy of the neural network. The optimal neural network structure for training and then predicting the performance of a fuel cell includes an identity activation function, a Limited Memory Broyden-Fletcher-Goldfarb-Shano algorithm solver (LBFGS) and at least five intermediate hidden layers. Fig. 15 presents a comparison between predicted values of power density in thirty cases obtained from various machine learning algorithms and the actual values obtained from numerical simulation. The results indicate that the power density of a solid oxide fuel cell operating with ammonia fuel can be accurately and reasonably approximated without the need for numerical or laboratory solutions.

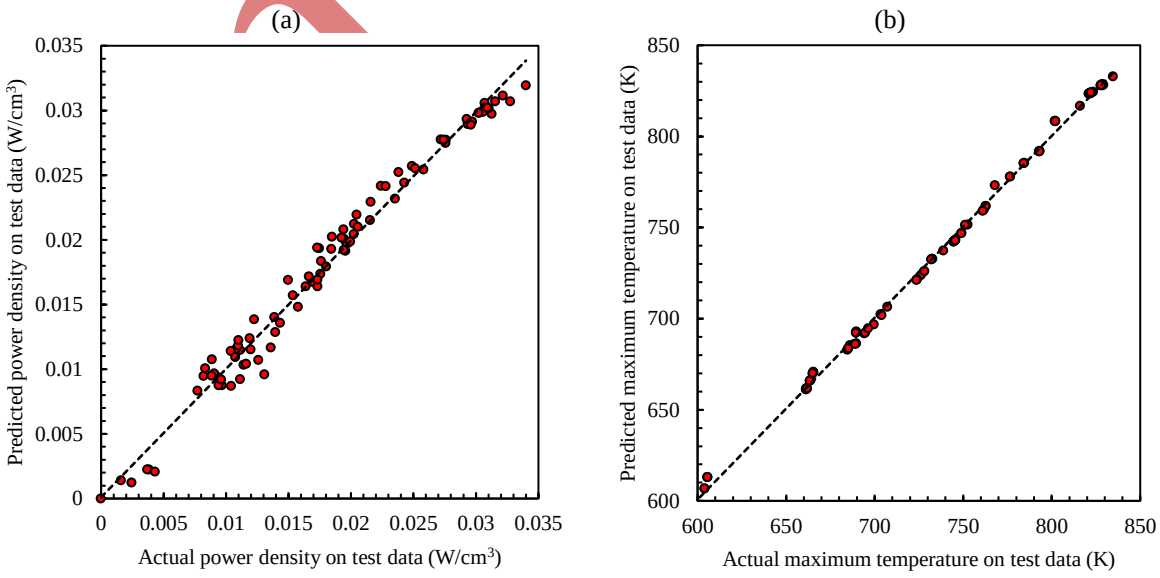

Fig. 14. Accuracy and performance of DNN in predicting a) power density and b) temperature.

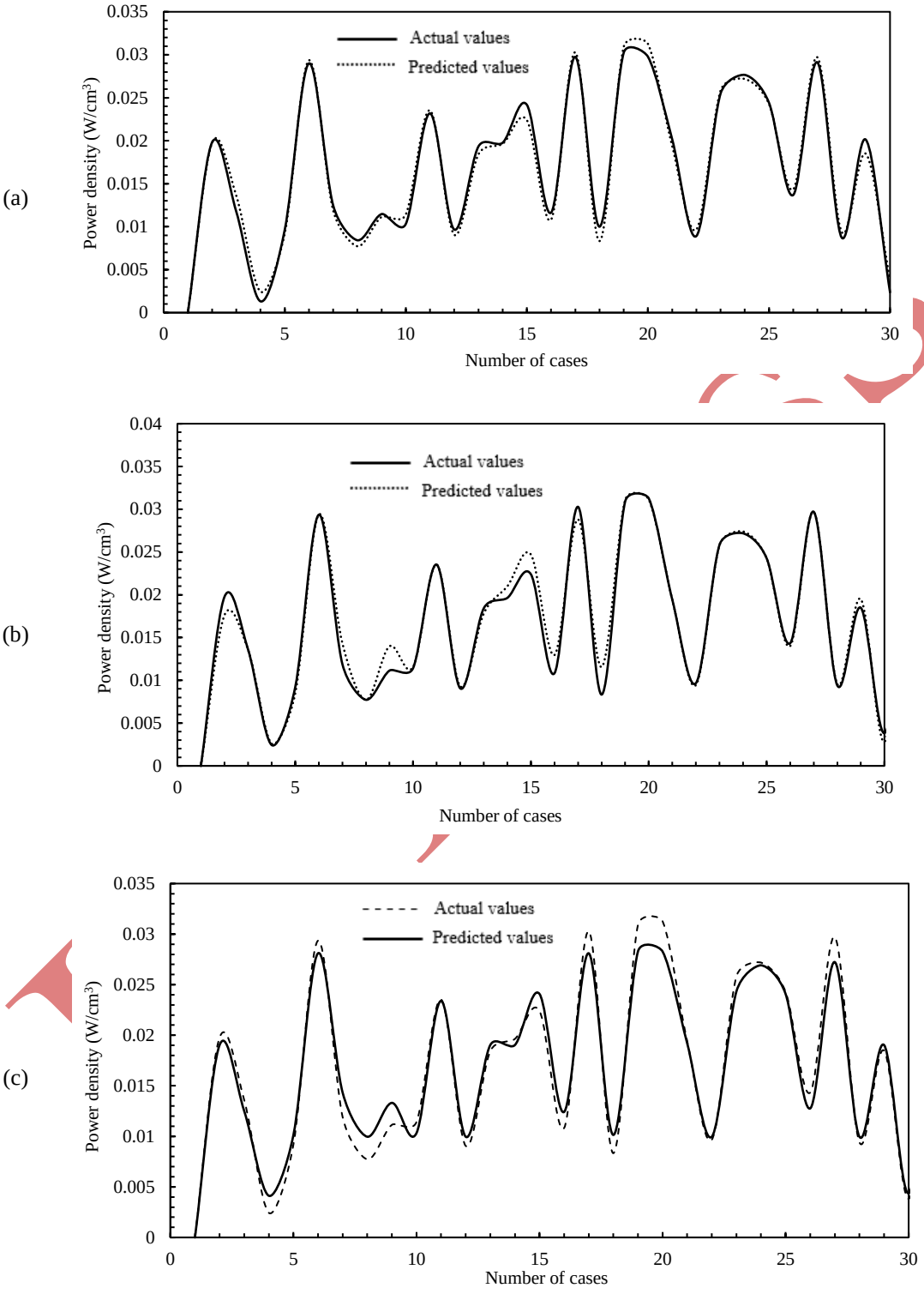

Fig. 15. Comparison chart of actual power density and predicted values by a) DNN, b) RFM and c) LASSO regression.

Fig. 16 illustrates the investigation and assessment of another objective parameter, namely the maximum temperature of the fuel cell. The precision of the machine's performance in forecasting the maximum temperature is notably high based on the findings. Furthermore, the results indicate a higher level of accuracy compared to the power density prediction model.

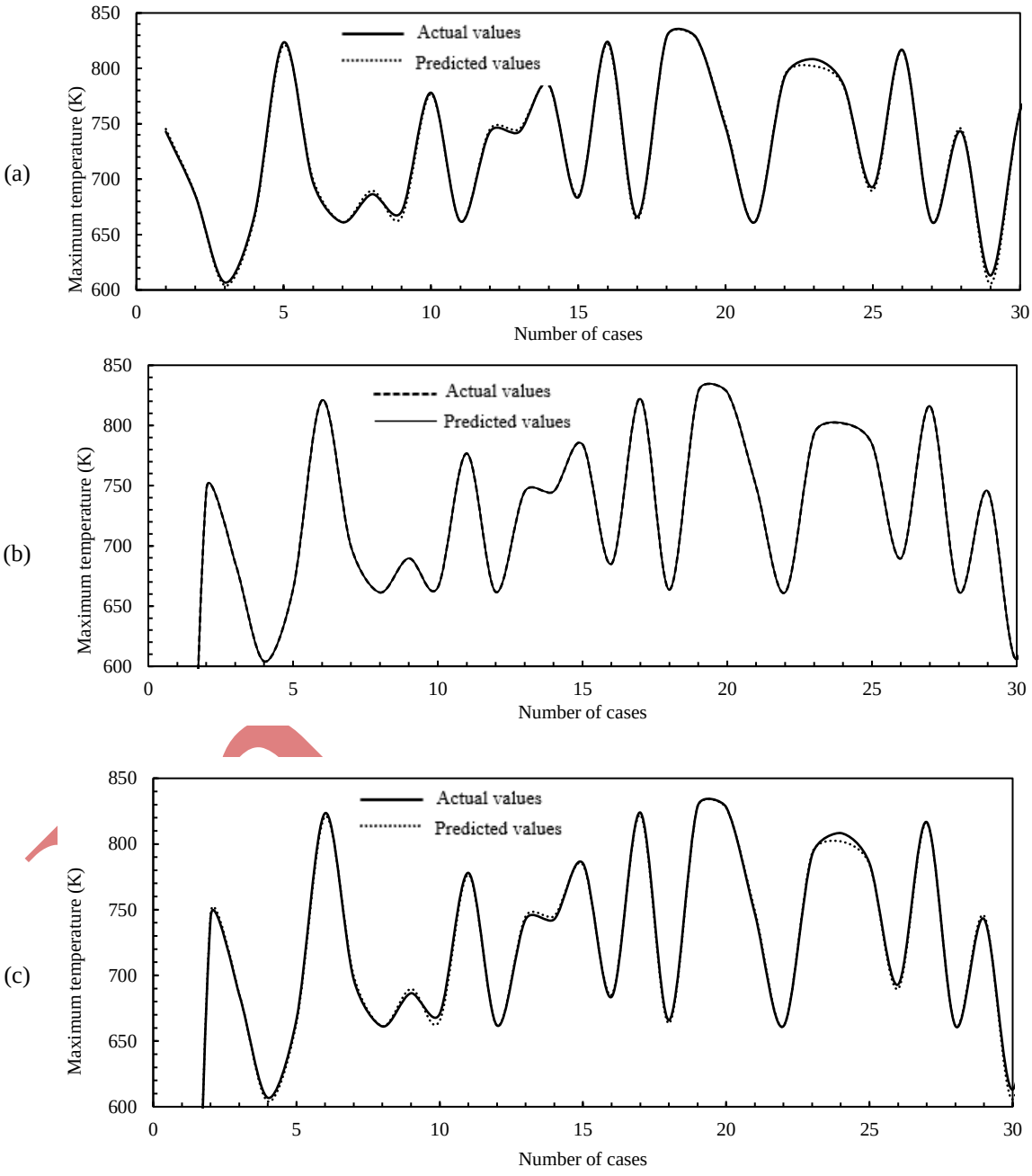

Fig. 16. Comparison chart of actual power density and predicted values by a) DNN, b) RFM and c) LASSO regression.

Table 2 displays the various errors associated with the algorithms used to predict power density and maximum temperature of the fuel cell. The Root Mean Square Error (RMSE), Mean Absolute Error (MAE), and Coefficient of Determination (R^2) show appropriate values for predicting the target parameters. The RFM and DNN algorithms have the highest accuracy in predicting the maximum temperature and power density of fuel cell, respectively. Additionally, considering that the R^2 value of DNN in this study is more than 98%, , compared to the results of other similar researches such as Milewski et al., Su et al. and Subotić et al. [32, 34, 39], it indicates the suitable performance of the machine in predicting the objective functions.

Table 2. Error-values and qualitative expressions of machine learning models in predicting objective functions.

Parameters	Model	RMSE_train	MAE_train	R^2_train	RMSE_test	MAE_test	R^2_test
Maximum temperature	RFM	0.000000	0.000000	1.000000	0.121286	0.088353	0.999996
Power density		0.000000	0.000000	1.000000	0.001152	0.000722	0.980176
Maximum temperature	DNN	2.613388	2.064174	0.997817	2.811718	2.156971	0.998046
Power density		0.001351	0.001091	0.96715	0.001093	0.000867	0.982156
Maximum temperature	LASSO	2.613389	2.064252	0.997817	2.812093	0.000874	0.998045
Power density		0.002015	0.001525	0.92695	0.0018	0.000874	0.951606

4. Conclusions

In this research, firstly, a tubular solid oxide fuel cell with ammonia fuel at intermediate operating temperature is simulated using Temkin-Pyzhev kinetic model. Then, considering the effects of variations in temperature, pressure, and mole fraction of species on thermophysical and fluid characteristics of flows, as well as thermal sources resulting from chemical and electrochemical reactions, the problem is solved steadily. To examine the two objective parameters, including the maximum temperature and power density of the fuel cell under different conditions, five input variables including inlet temperature, porosity of the cathode and anode, and the velocity of air and fuel flows are investigated and studied. In this regard, for 601 different modes, the finite element code is executed and solved by changing the input data. Considering the significant time cost and complexity of solving mass, momentum, energy, species and electric flux conservation equations, machine learning tools are used. To evaluate the performance of the machine in optimal and suitable prediction of the target terms, three algorithms including DNN, RF and Lasso regression are used, with implementation in the python programming language. The most important results of the current research are briefly stated below:

- Numerical analysis of the fuel cell shows that changing the inlet temperature has the most significant effect on the endothermic reaction of ammonia decomposition and as a result power generation in the fuel cell. It was also observed that along the length of the fuel cell, with the ammonia decomposition increases, the temperature decreases significantly.
- Investigating the correlation between the data using the Pearson Correlation Coefficient (P.C.C) method shows that the inlet temperature has the highest correlation with the target expressions of maximum temperature and fuel cell power density, with correlation coefficientsof 0.99 and 0.97, respectively.
- The most effective configuration for training a neural network to predict the performance of a fuel cell involves using the Identity

Activation Function, Limited- Memory Broyden–Fletcher–Goldfarb–Shanno (LBFGS) algorithm as solver, and incorporating at least five middle hidden layers take place.

- The highest level of accuracy in predicting the power density of a fuel cell is achieved using DNN, RF and Lasso Regression algorithms, respectively. Also, the R^2 values for the algorithms are 0.9822, 0.9802 and 0.9516, respectively. Results show that Lasso Regression is not as accurate as the other two algorithms in predicting the power density.
- The highest level of accuracy in predicting the maximum temperature of the fuel cell is achieved using DNN, RF and Lasso Regression algorithms, respectively. Also, the R^2 values for these three algorithms are 0.9999, 0.9980 and 0.9980, respectively. The results show that the prediction of the maximum temperature of the fuel cell with three algorithms is done with appropriate accuracy with RF having the most proper performance among all three algorithms.

References

[1] Y. Wang, Y. Gu, H. Zhang, J. Yang, J. Wang, W. Guan, J. Chen, B. Chi, L. Jia, H. muroyama, T. Matsui, K. Eguchi and Z. Zhong, "Efficient and durable ammonia power generation by symmetric flat-tube solid oxide fuel cells", *Appl. Energy*, Vol. 270, p. 115185, (2020).

[2] R. Braun and P. Kazempoor, "Application of SOFCs in combined heat, cooling and power systems", *Solid Oxide Fuel Cells: From Materials to System Modeling*, Eds. M. Ni and T. S. Zhao, pp.327-381, (2013).

[3] M. Liu, A. Lanzini, W. Halliop, V. Cobas, A. Verkooijen and P. Aravind, "Anode recirculation behavior of a solid oxide fuel cell system: A safety analysis and a performance optimization", *Int. J. Hydrogen Energy*, Vol. 38, No. 6, pp. 2868-2883, (2013).

[4] J. Yang, T. Akagi, T. Okanishi, H. Muroyama, T. Matsui and K. Eguchi, "Catalytic Influence of Oxide Component in Ni-Based Cermet Anodes for Ammonia-Fueled Solid Oxide Fuel Cells", *Fuel Cells*, Vol. 15, No. 2, pp. 390-397, (2015).

[5] G. Cinti, U. Desideri, D. Penchini and G. Discepoli, "Experimental analysis of SOFC fuelled by ammonia", *Fuel Cells*, Vol. 14, No. 2, pp. 221-230, (2014).

[6] N. Jantakananuruk, *Performance, Temperature and Concentration Profiles in a Non-Isothermal Ammonia-Fueled Tubular SOFC*, Master thesis, Worcester Polytechnic Institute, Worcester, Massachusetts, (2019).

[7] M. Asmare and M. İlbaş, "Direct ammonia fueled solid oxide fuel cells: A comprehensive review on challenges, opportunities and future outlooks", *Int. J. Energy T.*, Vol. 2, No. 1, (2020).

[8] A. Wojcik, H. Middleton and I. Damopoulos, "Ammonia as a fuel in solid oxide fuel cells", *J. Power Sources*, Vol. [9] E. S. M. Seo, W. K. Yoshito, V. Ussui, D. R. R. Lazar, S. R. H. d. M. Castanho and J. O. A. Paschoal, "Influence of the starting materials on performance of high temperature oxide fuel cells devices", *Mater. Res.*, Vol. 7, pp. 215-220, (2004).

[10] F. Ishak, I. Dincer and C. Zamfirescu, "Thermodynamic analysis of ammonia-fed solid oxide fuel cells", *J. Power Sources*, Vol. 202, pp. 157-165, (2012).

[11] S. A. Hajimolana, M. A. Hussain, W. W. Daud and M. Chakrabarti, "Dynamic modelling and sensitivity analysis of a tubular SOFC fuelled with NH3 as a possible replacement for H2", *Chem. Eng. Res. Des.*, Vol. 90, No. 11, pp. 1871-1882, (2012).

[12] O. Siddiqui and I. Dincer, "A review and comparative assessment of direct ammonia fuel cells", *Therm. Sci. Eng. Prog.*, Vol. 5, pp. 568-578, (2018).

[13] K. Machaj, M. Skrzypkiewicz, A. Niemczyk, J. Kupecki, Z. Malecha and M. Chorowski, "Impact of Thickness on Direct Ammonia Decomposition in Solid Oxide Fuel Cells, Numerical and Experimental Research", *ECS Trans.*, Vol. 111, No. 6, p. 2203, (2023).

[14] M. Ilbas, B. Kumuk, M. A. Alemu and B. Arslan, "Numerical investigation of a direct

ammonia tubular solid oxide fuel cell in comparison with hydrogen", *Int. J. Hydrogen Energy*, Vol. 45, No. 60, pp. 35108-35117, (2020).

[15] A. F. S. Molouk, J. Yang, T. Okanishi, H. Muroyama, T. Matsui and K. Eguchi, "Comparative study on ammonia oxidation over Ni-based cermet anodes for solid oxide fuel cells", *J. Power Sources*, Vol. 305, pp. 72-79, (2016).

[16] L. Barelli, G. Bidini and G. Cinti, "Operation of a solid oxide fuel cell based power system with ammonia as a fuel: Experimental test and system design", *Energies*, Vol. 13, No. 23, p. 6173, (2020).

[17] M. Ilbas, M. A. Alemu and F. M. Cimen, "Comparative performance analysis of a direct ammonia-fuelled anode supported flat tubular solid oxide fuel cell: a 3D numerical study", *Int. J. Hydrogen Energy*, Vol. 47, No. 5, pp. 3416-3428, (2022).

[18] M. Asmare, M. Ilbas, F. M. Cimen, C. Timurkutluk and S. Onbilgin, "Three-dimensional numerical simulation and experimentalvalidation on ammonia and hydrogen fueled micro tubular solid oxide fuel cell performance", *Int. J. Hydrogen Energy*, Vol. 47, No. 35, pp. 15865-15874, (2022).

[19] M. Keyhanpour and M. Ghasemi, "3D Investigation of Tubular PEM Fuel Cell Performance Assuming Fluid-Solid-Heat Interaction", *J. Comp. Methods Eng.*, Vol. 41, No. 1, pp. 79-99, (2022).

[20] M. Keyhanpour and M. Ghasemi, "3D Simulation of Effect of Geometry and Temperature Distribution on SOFC Performance", *J. Fluid Mech. Aerodyn.*, Vol. 10, No. 2, pp. 169-184, (2022).

[21] S. A. Vilekar, I. Fishtik and R. Datta, "The peculiar catalytic sequence of the ammonia decomposition reaction and its steady-state kinetics", *Chem. Eng. Sci.*, Vol. 71, pp. 333-344, (2012).

[22] J. Badur, M. Lemański, T. Kowalczyk, P. Ziółkowski and S. Kornet, "Zero-dimensional robust model of an SOFC with internal reforming for hybrid energy cycles", *Energy*, Vol. 158, pp. 128-138, (2018).

[23] J. Kupecki, D. Papurello, A. Lanzini, Y. Naumovich, K. Motylinski, M. Blesznowski and M. Santarelli, "Numerical model of planar anode supported solid oxide fuel cell fed with fuel containing H2S operated in direct internal reforming mode (DIR-SOFC)", *Appl. Energy*, Vol. 230, pp. 1573-1584, (2018).

[24] L. Barelli, G. Bidini, G. Cinti and A. Ottaviano, "Studyof SOFC-SOE transition on a RSOFC stack", *Int. J. Hydrogen Energy*, Vol. 42, No. 41, pp. 26037-26047, (2017).

[25] G. Botta, M. Romeo, A. Fernandes, S. Trabucchi and P. Aravind, "Dynamic modeling of reversible solid oxide cell stack and control strategy development", *Energy Convers. Manage.*, Vol. 185, pp. 636-653, (2019).

[26] V. Menon, V. M. Janardhanan and O.Deutschmann, "A mathematical model to analyze solid oxide electrolyzer cells (SOECs) for hydrogen production", *Chem. Eng. Sci.*, Vol. 110, pp. 83-93, (2014).

[27] N. Chowdhury and G. Chandra Deka, *Multidisciplinary Functions of Blockchain Technology in AI and IoT Applications: IGI Global*, Ministry of Skill Development and Entrepreneurship, New Delhi, pp. 1-255, (2020).

[28] B. Yang, Z. Guo, Y. Yang, Y. Chen, R. Zhang, K. Su, H. Shu, T. Yu and X. Zhang, "Extreme learning machine based meta-heuristicalgorithms for parameter extraction of solid oxide fuel cells", *Appl. Energy*, Vol. 303, p. 117630, (2021).

[29] R. Ding, Y. Ding, H. Zhang, W. Yin, R. Wang, Z. Xu, Y. Liu, J. Wang, J. Li and J. Liu, "Applying machine learning to boost thedevelopment of high-performance membrane electrode assembly for proton exchange membrane fuel cells", *J. Mater. Chem. A*, Vol. 9, No. 11, pp. 6841-6850, (2021).

[30] Q. Zhao and X. Tang, "Prediction of battery performance degradation based on machine learning", *Second Int. Conf. Sustainable Technology and Management* (*ICSTM*), Vol. 12804: SPIE, pp. 221-229, (2023).

[31] J. Arriagada, P. Olausson and A. Selimovic, "Artificial neural network simulator for SOFC performance prediction", *J. Power Sources*, V. 112, No. 1, pp. 54-60, (2002).
[32] J. Milewski and K. Świrski, "Modelling the SOFC behaviours by artificial neural network", *Int. J. Hydrogen Energy*, Vol. 34, No. 13, pp. 5546-5553, (2009).
[33] K. Chaichana, Y. Patcharavorachot, B. Chutichai, D. Saebea, S. Assabumrungrat and A. Arpornwichanop, "Neural network hybrid model of a direct internal reforming solid oxide fuel cell", *Int. J. Hydrogen Energy*, Vol. 37, No. 3, pp. 2498-2508, (2012).
[34] H. Xu, J. Ma, P. Tan, B. Chen, Z. Wu, Y. Zhang, H. Wang, J. Xuan and M. Ni, "Towards online optimisation of solidoxide fuel cell performance: Combining deep learning with multi-physics simulation", *Energy AI*, Vol. 1, p. 100003, (2020).
[35] F. C. İskenderoğlu, M. K. Baltacioğlu, M. H. Demir, A. Baldinelli, L. Barelli, and G. Bidini, "Comparison of support vector regressionand random forest algorithms for estimating the SOFC output voltage by considering hydrogen flow rates", *Int. J. Hydrogen Energy*, Vol. 45, No. 60, pp. 35023-35038, (2020).
[36] S. Ba, D. Xia and E. M. Gibbons, "Model identification and strategy application for Solid Oxide Fuel Cell using Rotor HopfieldNeural Network based on a novel optimization method", *Int. J. Hydrogen Energy*, Vol. 45, No. 51, pp. 27694-27704, (2020).
[37] J. Li and T. Yu, "A novel data-driven controller for solid oxide fuel cell via deep reinforcementlearning", *J. Cleaner Prod.* , Vol. 321, p. 128929, (2021).
[38] H. Jia and B. Taheri, "Model identification of solid oxide fuel cell using hybrid Elman neuralnetwork/quantum pathfinder algorithm", *Energy Rep.*, Vol. 7, pp. 3328-3337, (2021).
[39] V. Subotić, M. Eibl and C. Hochenauer, "Artificial intelligence for time-efficient predictionand optimization of solid oxide fuel cell performances", *Energy Convers. Manage.*, Vol. 230, p. 113764, (2021).
[40] F. Mütter, C. Berger, B. Königshofer, M. Höber, C. Hochenauer and V. Subotić,"Artificial intelligence for solid oxide fuel cells: Combining automated high accuracy artificial neural network model generation and genetic algorithm for time-efficient performance prediction and optimization", *Energy Convers. Manage.*, Vol. 291, p. 117263, (2023).
[41] M. Tofigh, Z. Salehi, A. Kharazmi, D. J. Smith, A. R. Hanifi, C. R. Cokh and M. Shahbakhti, "Transient modeling of a solid oxide fuel cell using an efficient deep learning HY-CNN-NARX paradigm", *J. Power Sources*, Vol. 606, p. 234555, (2024).
[42] H. Kim, J. Lee, A. Gokbayrak, Y. Seo, S. Oh, M. Oh, Y. Jun, J. Son and S. Yang, "Characterization of direct-ammonia solid oxide fuel cells (DA-SOFCs) at 650–750° C in a single-repeating unit stack: Effects of metallic components and residual ammonia", *Int. J. Hydrogen Energy*, Vol. 68, pp. 1312-1321, (2024).
[43] Z. Gong, H. Wang, C. Li, Q. Sang, Y. Xie, X. Zhang and Y. Liu, "Progress in the design and performance evaluation of catalystsfor low-temperature direct ammonia fuel cells", *Green Chem. Eng.*, pp. 1-14, (2024).
[44] S. N. Ranasinghe and P. H. Middleton, "Modelling of single cell solid oxide fuel cellsusing COMSOL multiphysics", *2017 IEEE Int. Conf. Environ. Elec. Eng. 2017 IEEE Indus. Com. Power Sys. Europe (EEEIC/I&CPS Europe)*, pp. 1-6, (2017).
[45] D. F. Cheddie, "Temkin-Pyzhev kinetics in intermediate temperature ammonia-fed solid oxide fuel cells", *Int. J. PowerEnergy Res.*, Vol. 2, No. 3, pp. 43-51, (2018).
[46] M. Keyhanpour, M. Ghassemi and M. Pourbagian, "Parametric Study of Ammonia-Fueled Tubular AP-SOFC with Temkin-Pyzhev Kinetic Model", *J. Iranian Chem. Eng.*, Vol. 22, No. 129, pp. 110-123, (2023).
[47] D. Su, J. Zheng, J. Ma, Z. Dong, Z. Chen and Y. Qin, "Application of Machine Learningin Fuel Cell Research", *Energies*, Vol. 16, No. 11, p. 4390, (2023).
[48] M. H. Golbabaei, M. R. Saeidi Varnoosfaderani, A. Zare, H. Salari, F.

Hemmati, H. Abdoli and B. Hamawandi, “Performance Analysis of Anode-Supported Solid Oxide Fuel Cells: A Machine Learning Approach”, *Materials*, Vol. 15, No. 21, p. 7760, (2022).

[49] S. Wang, Y. Chen, Z. Cui, L. Lin and Y. Zong, “Diabetes RiskAnalysis Based on Machine Learning LASSO Regression Model”, *J. Theory and Practice Eng. Sci*., Vol. 4, No. 01, pp. 58-64, (2024).